European Journal of Mechanics / A Solids 116 (2026) 105858

Contents lists available at ScienceDirect

European Journal of Mechanics / A Solids

journal homepage: www.elsevier.com/locate/ejmsol

Full length article

Additive manufacturing of a transtibial prosthetic socket through a FE-based topology optimization approach

Cristina Falcinelli [a,*], Iacopo Bianchi [b], Alessia Carugno [a], Archimede Forcellese [b]

[a] Department of Engineering and Geology, University G d'Annunzio Chieti-Pescara, Pescara, Italy
[b] Department of Industrial Engineering and Mathematical Science, Università Politecnica delle Marche, Ancona, Italy

ARTICLE INFO

Keywords:
Topology optimization
Finite element method
3D printing
Prosthetic socket

ABSTRACT

The present work explores the possibility of combining 3D printing and topology optimization to produce lightweight transtibial prosthetic sockets to reduce the manufacturing time, costs and material waste. Specifically, a topology optimization algorithm based on Finite Element (FE) method has been employed to determine the optimal material distribution for the prosthetic socket in Polyamide PA12. A FE analysis has been carried out to validate the behaviour of the optimized shape. Finally, the new shape has been 3D printed using the fused deposition modelling technology. Furthermore, a cost analysis has been performed on the 3D printed part and traditional prosthetic socket. The approach followed in the present work showed a time reduction of up to 50% for the production of the final prosthesis and a cost reduction of up to 80% compared to the traditional manufacturing process. Moreover, the optimization of the material distribution allows for a reduction of material use (i.e. −38%). This procedure demonstrates the potential of the proposed approach for developing an efficient and sustainable alternative in the manufacturing of prosthetic sockets.

1. Introduction

A prosthetic socket is a medical device that connects the residual limb with the prosthesis and its aim is to guarantee an integration of the prosthesis as a functional extension of the body (Zhang et al., 1998). Traditionally, prosthetic sockets are produced via a manual and complicated manufacturing process. Wang et al. (2020) described the traditional manufacturing process for producing a prosthetic socket. First, the prosthetic socket is fabricated using a thermoplastic material to accommodate the changes in volume of the residual limb. In detail, a cast mold is obtained by wrapping plaster bandages around the residual limb. A positive mold is then made by pouring plaster into the negative cast mold. Next, the prosthetic socket is made by heating and vacuum-forming sheets of thermoplastic onto the positive plaster mold, which are left to cool down. Finally, some manual shape modifications are made to guarantee a proper load distribution between the prosthesis and the residual limb during walking or other activities to reduce the risk of discomfort or skin damage.

The traditional manufacturing process can involve the production of two devices: a temporary prosthetic socket and a final prosthetic socket. The temporary prosthetic socket, which is manufactured following the steps described above, is commonly worn for 3–6 months. After this period, a final prosthetic socket is manufactured based on the positive mold created for the temporary prosthesis performing some manual modifications to adapt it to the residual limb. This final prosthesis is then finalized by pouring it with carbon material.

The whole manufacturing process results in the waste of materials and has high time and labor costs (Wang et al., 2020). Moreover, the quality of the product is extremely dependent on the skill and experience of the technician. In the view of overcoming such drawbacks, additive manufacturing (AM) in combination with finite element (FE)-based topology optimization (TO) may represent an alternative way to design and produce prosthetic sockets.

AM is a layered manufacturing technique that creates objects from tridimensional (3D) data, using digitally controlled and operated material laying tools (Tom et al., 2022; Di Pompeo et al., 2021; Forcellese et al., 2022). Compared with conventional manufacturing techniques, AM greatly reduces material waste, shortens the fabrication period, and eliminates the need for most skill-based manual operations (Attaran, 2017; Iftekar et al., 2023). Moreover, AM offers the advantages to manufacture complex structures and realize the parts with a high degree of customization. Due to these advantages, in recent years, AM has been applied for several biomedical applications (Meng et al., 2023; Singh and Ramakrishna, 2017; Zhang et al., 2023; Kumar et al., 2021).

In the field of prosthetic socket, some studies have demonstrated the advantages in using AM such as the production of lightweight and

* Corresponding author.
E-mail address: cristina.falcinelli@unich.it (C. Falcinelli).

https://doi.org/10.1016/j.euromechsol.2025.105858
Received 7 January 2025; Received in revised form 1 September 2025; Accepted 1 September 2025
Available online 8 September 2025
0997-7538/© 2025 The Authors. Published by Elsevier Masson SAS. This is an open access article under the CC BY license (http://creativecommons.org/licenses/by/4.0/).

more comfortable devices with the possibility to adjust the socket to fit the individual's residual limb (Vitali et al., 2017; Pourfarzaneh et al., 2019). In the study performed by Van Der Stelt et al. (2021), transtibial prosthetic sockets have been manufactured with Fused Deposition Modelling (FDM) as 3D printing technique using polylactic acid (PLA) with the following printing parameters: 0.80 mm nozzle diameter, 100% infill, 0.2 mm layer thickness, and 45 mm/s speed. The Authors obtained 3D-printed sockets weighing approximately 1560 g, which is less than the weight of the conventionally manufactured socket, which weighed 1945 g. These sockets have been tested on subjects of a rural area of Sierra Leone that indicated that lightweight prostheses provide more comfort while wearing it. Pourfarzaneh et al. (2019) proposed the way of 3D printing prosthetic sockets using variable stiffness shape memory/lattice structure leading to create an adaptive device to obtain a more comfortable and better fitting socket. These works proved the feasibility of using AM to produce prosthesis, with advantages in terms of weight reduction, adaptability and increased comfort for the patients. However, they do not explore in depth the advantages in terms of design complexity offered by the innovative technology. To fully exploit the ability of AM to produce complex geometries, it is required to move beyond the current state of the art by integrating structural considerations and design optimization for the development of prosthetic sockets.

FE-based TO is a numerical method to find the best material distribution of a structure within a specific domain to obtain desired properties while satisfying prescribed constraints with the advantages of minimizing waste and cost savings in material and manufacturing process (Sigmund and Maute, 2013; Li et al., 2020; Almeida and Bártolo, 2013; Sutradhar et al., 2010). In addition, FE-based TO allows the design of patient-specific wearable devices such as transtibial prosthetic sockets with the advantage of saving weight and improving the comfort. Nayak et al. (2017) employed the TO technique to identify potential structural designs for minimizing mass and enhancing the performance of the transtibial prosthetic socket concluding that their results may provide significant insights into the socket design and a roadmap for customization of the sockets. In the study performed by Norli et al. (2024), potential improvements of the transtibial prosthetic socket design have been investigated through TO analysing 5 different optimized designs. The mechanical performance of these designs has been evaluated under static analysis in terms of stress distribution. The Authors demonstrated that each design guaranteed a reduction in weight, resulting in different stress patterns that could potentially improve patient comfort.

Due to all these advantages, recently the combination of the AM and TO started to represent a promising approach to developing innovative structures with high performance, finding many applications in different fields such as aerospace, automotive, construction and medicine (Prathyusha and Raghu Babu, 2022). Among these, biomedical applications are particularly attractive, as the combination of AM and TO enables the design and development of patient-specific devices and solutions (Li et al., 2020; Moussa et al., 2020; Hu et al., 2019; Smit et al., 2023; Zoboli et al., 2024). To the best of the Authors' knowledge, there are no studies in the literature that have investigated the possibility to use both the AM and TO to manufacture transtibial prosthetic sockets. As such, the aim of the present work is to perform a first exploratory work in which a FE-based TO approach is used to find an optimal pattern for the material distribution within a transtibial prosthetic socket. Then, a validation analysis is performed to confirm the stress and displacement distributions of the optimized shape. Finally, the optimized design is manufactured through AM to evaluate the manufacturing time and cost and compare the innovative solution costs with the traditional alternative.

Fig. 1. Transtibial prosthetic socket manufactured through conventional technique: the positive mold made by pouring plaster into the negative cast mold (on the left) and the final transtibial socket (on the right).

2. Material and methods

In the present study, a prosthetic socket manufactured using conventional technique for a male patient, 66 years old, 168 cm in height, 52 kg, with amputation at the left side, has been analysed. The manufacturing of the prosthetic socket with conventional technique has taken 2 days. In Fig. 1 the transtibial prosthetic socket obtained through the conventional manufacturing process is shown.

2.1. Computational modelling

Geometry. Once the prosthetic socket was manufactured, it was scanned using the Occipital System SA38 to reconstruct the 3D geometry. The scanning procedure generated an object (OBJ) file, which was then converted into Standard Triangulation Language (STL) format using the open-source 3D modelling software Meshmixer (Meshmixer 3.5, Autodesk Inc., San Rafael, CA, USA). Then, the STL of the socket was imported in Siemens NX (Release 2023) to create the geometry of the residual limb in contact with the socket to account for the presence of the soft tissues in the model. Specifically, using the Reverse Engineering module, some CAD modelling operations, such as extrusion and boolean difference, were applied to the prosthetic socket to obtain the final geometry of the residual limb. Finally, the 3D geometries of both prosthetic socket and residual limb have been imported within the FE simulation environment Comsol Multiphysics for the static structural analysis. Fig. 2 shows the geometries of prosthetic socket and residual limb, along with the final assembled geometry.

It is important to highlight that in practical implementation of the proposed framework, the scan would be acquired directly from the residual limb of the patient. However, in this work, the conventionally manufactured socket has been scanned to simplify the development process and avoid delays associated with the formal consent procedures required for scanning human subjects.

Computational discretization. Computational mesh was created through second-order displacement-based tetrahedral elements, resulting in unstructured topology (Fig. 3). The mesh has been carefully designed, and both the mesh size and refinement level have been determined through a preliminary convergence analysis, which is discussed in detail in Section 3.1.

Constitutive description. The constitutive behaviour of both the prosthetic socket and the residual limb was assumed to be linear, elastic, isotropic and homogeneous. For the residual limb, the Young's modulus E_{rl} and the Poisson's ratio ν_{rl} used in the present work are reported

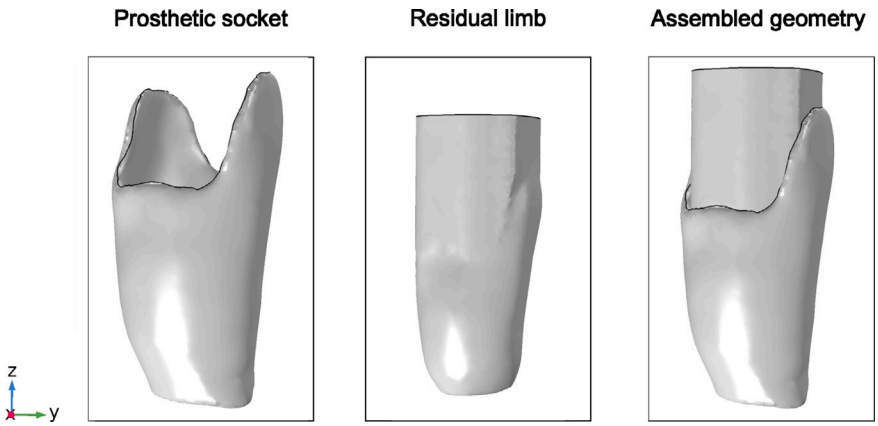

Fig. 2. The 3D geometries of prosthetic socket and residual limb, and the final 3D assembled geometry.

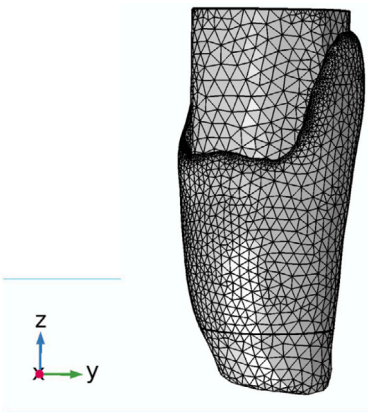

Fig. 3. Unstructured tetrahedral mesh for the transtibial prosthetic socket and the residual limb.

Table 1
Elastic properties of residual limb and PA12.

Material	Young's modulus (MPa)	Poisson's ratio
Residual limb	0.2[a]	0.49[a]
PA12	1029[b]	0.4[c]

[a] Jia et al. (2004).
[b] Tomanik et al. (2021).
[c] Amado-Becker et al. (2008).

in Table 1. For the prosthetic socket, the Polyamide PA12 (or Nylon) has been analysed. PA12 is a technical thermoplastic material and it is commonly used due to its noteworthy mechanical, thermal and electrical properties (Zárybnická et al., 2022; Vidakis et al., 2022). These characteristics, along with its biocompatible nature, make PA12 an optimal solution for biomedical applications; some examples are dental implants, biomedical devices, scaffolds for bone growth and orthopaedic prostheses (Nakonieczny et al., 2021; Shakiba et al., 2021). In addition, PA12 can be used in different 3D printing technologies such as fused deposition modelling (FDM) and selective laser sintering (SLS); hence, it results in an optimal solution for customized and complex-shaped orthoses (Ejnisman et al., 2021; Abas et al., 2023). The material data of PA12 (i.e., the Young's Modulus E_s and Poisson's ratio ν_s) used in this work are listed in Table 1. It is important to highlight that the values of the material properties for PA12 have been chosen in accordance with the material specifications provided by the manufacturer Sinterit.

2.2. Topology optimization

Topology optimization combines numerical methods such as FE method with optimization algorithms to determine the optimal distribution of a given amount of material within a prescribed design domain, aiming to achieve the best structural performance (Sigmund and Maute, 2013).

Let consider Ω the design domain and a discretization in finite elements of Ω. In case of the density approach of topology optimization in which the design variable is the element-wise density, the problem design can be expressed by the following relations:

$$\min_{\rho} G(\mathbf{u}(\boldsymbol{\rho}), \boldsymbol{\rho}) = \sum_{i=1}^{N} \int_{\Omega_i} g(\mathbf{u}(\rho_i), \rho_i)\, dV \tag{1}$$

$$\text{such that: } F_0(\boldsymbol{\rho}) = \sum_{i=1}^{N} v_i \rho_i - V_0 \leq 0, \tag{2}$$

$$0 \leq \rho_i \leq 1, \quad i = 1, \ldots, N \tag{3}$$

where G is the objective function to minimize, $\mathbf{u}$ the displacement field vector, N the total number of finite elements and $\boldsymbol{\rho}$ the density vector of length N. Eq. (2) represents the volume constraint with v_i the volume of the i-th finite element with associated density ρ_i, V_0 and F_0 the initial and final volume of the design domain. Eq. (3) indicates the values that the density variable can assume. In detail, a value close to 1 indicates that the material is needed and should be kept, whereas a value close to zero suggests that it can be removed. The function $g(\boldsymbol{u}(\rho_i), \rho_i)$ represents the interpolation between density and material property and can be written as

$$g(\boldsymbol{u}(\rho_i), \rho_i) = g(\rho_i) f_0(\mathbf{u}) \tag{4}$$

with $g(\rho_i)$ the density interpolation function and $f_0(\mathbf{u})$ a function of the field for solid material (i.e. the strain energy density in case of a compliance objective). The Eqs. (1), (2) and (3) represent the discretized topology optimization formulation with a continuous design variable. One approach to solve this kind of problem is to implement the Solid Isotropic Material with Penalisation (SIMP) method. In the SIMP approach the relation between the density design variable and the material property for each element is given by the following power-law:

$$E(\rho_i) = \rho_i^p E_0 \tag{5}$$

with p the penalization parameter and E_0 the original Young's modulus of the material in the solid phase corresponding to the density equal to 1. The penalization parameter p is used to reduce the contribution of elements with intermediate densities to the total stiffness steering the optimized solution to elements that are either solid or void. As indicated by numerical experiments (Sigmund and Maute, 2013; Bendsøe

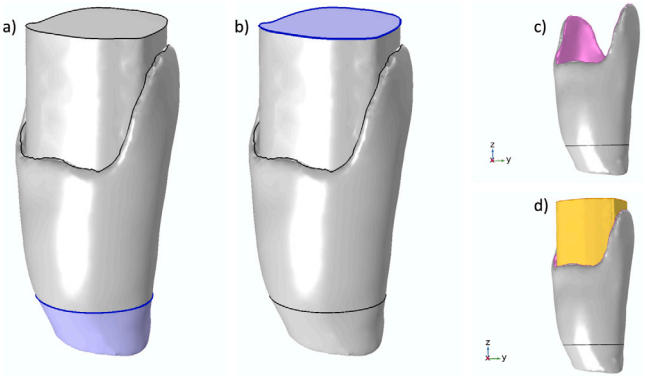

Fig. 4. Boundary conditions adopted in the present study: (a) region fully constrained; (b) surface where the pressure is applied; (c) and (d) surfaces (in yellow and magenta) where the bonded contact has been applied.

and Sigmund, 1999), $p = 3$ ensures a convenient convergence of the solution to density values of either 0 or 1 (i.e., reducing the number of elements with intermediate values of topology density). According to Eq. (5), the elastic modulus of an element is reduced leading to a reduction of element stiffness. Accordingly, the global stiffness matrix ($\mathbf{K}_{\text{global}}$) can be expressed as:

$$\mathbf{K}_{\text{global}} = \sum_{i=1}^{N} \left[\rho_{\min} + (1 - \rho_{\min})\rho_i^p\right] \mathbf{K}_i \tag{6}$$

where $\mathbf{K}_i$ is the element stiffness matrix and $\rho_{\min}$ is the minimum value of density used for stability reasons and to prevent singularity of the stiffness matrix.

In general, a TO algorithm based on FE analysis consists of two phases: a static analysis and an iterative procedure. As will be clarified in the following Sections, the first phase aims to compute the stress and strain distribution as well as the starting value of the objective function under predefined loading conditions. Then, during the second phase an iterative procedure is implemented with the aim of distributing the mass to satisfy the objective function and constraints.

Static structural analysis. In the static analysis, the bottom surface of the prosthetic socket has been considered fully constrained (displacement vector equal to zero, $\mathbf{u} = 0$) (Fig. 4a) whereas a pressure of 0.4 kPa has been applied on the top surface of the residual limb (Figs. 4a and 4b). Moreover, bonded contact has been considered on the contact surfaces between the residual limb and prosthetic socket (Figs. 4c and 4d). The choice of considering fully constrained the distal end of the prosthetic socket was based on the mechanical behaviour of the distal interface of the socket. The residual limb is inserted into the proximal end of the prosthetic socket, whereas distally, the socket is connected to the pylon or adapter which in turn connects to the prosthetic foot or other distal components. During both static and dynamic conditions loads are transmitted from the residual limb through the socket to the ground via the adapter, pylon, and foot. At the distal interface between the socket and adapter, relative motion is mechanically constrained due to the rigid fixation (Jindal et al., 2025). The main role of this interface is to enable structural load transfer. Therefore, in the static analysis, the distal end was modelled as fully constrained to accurately reflect its mechanical behaviour and enable realistic simulation of load transmission. In terms of load, given the area of load application, the pressure load of 0.4 kPa was equivalent to an approximate total load of 30 N. It is important to highlight that in the present work the load value of 30 N is used as an example load for performing topology optimization and comparing stress and displacement distributions before and after optimization. It does not represent a physiological loading condition.

Iterative procedure. Once the static analysis has been performed, a FE-based iterative procedure has been developed and implemented to find the mass distribution that satisfies the objective function and constraints. In the present work, the total strain energy has been chosen as the objective function. The transtibial prosthetic socket has been considered the domain to optimize and a reduction of 50% of the mass has been prescribed. Moreover, the minimum value of topology density $\rho_{\min}$ has been set equal to 0.001 (Sutradhar et al., 2010). Furthermore, to avoid the presence of too many elements with intermediate values of topology density, and consequently to obtain a clearer optimized design pattern, the SIMP has been used with a penalty factor equal to 3.

2.3. 3D printing

To validate the possibility of using AM for the production of the prosthetic socket and to thoroughly assess the proposed solution, the optimized component was produced using a FDM 3D printing machine. Among the possible techniques available for PA12 printing, FDM was selected as it is an easy and clean process to carry out and, due to its broad diffusion, it has low cost (Kumar et al., 2024). The Ultimaker s7 printer was employed to manufacture the optimized socket using PA12 filament as raw material. The .stl file obtained via TO was imported in the Cura slicing software to select the process parameters and create the part program. More specifically, a printing speed of 70 mm/s, a layer height equal to 0.25 mm, a nozzle diameter of 0.4 mm, an extrusion temperature equal to 260 °C and a bed temperature of 80 °C were selected. Printing temperatures (i.e. nozzle and build platform) were selected considering typical recommended values for PA12 in line with previous literature works concerning FDM 3D printing (Almuflih et al., 2024; Kam et al., 2021). The selected layer height and nozzle diameter are standard values in FDM 3D printing (Chojnacki et al., 2025) as they provide a good compromise between parts resolution and printing time. Similarly, the printing speed was selected to maintain dimensional accuracy whilst limiting printing time (Abas et al., 2022).

2.4. Cost assessment

A cost evaluation was conducted to compare the costs of the innovative solution with those of the traditional alternative, accounting for both temporary and final prosthetic socket production processes (Fig. 5).

- Traditional temporary socket: This scenario includes the negative cast mold creation by applying plaster bandages over the patient's residual limb. Hence, plaster is poured over the negative mold to recreate the residual limb. The socket is then produced via thermoforming by heating and softening a sheet of thermoplastic material and draping it onto the plaster model. Trimming and other finishing operations are required before assembling the socket with the other prosthetic components.
- Traditional final socket: Starting from the temporary prosthesis, a positive mold is created by casting plaster within the provisional socket. Tubular carbon fiber (CF) sleeves are manually placed over the plaster mold and a thermosetting resin is evenly poured over the sleeve. Multiple CF woven fabric layers are applied over the mold to ensure the desired mechanical properties; this also allows to apply foam and install adapters to assembly the socket and the other prosthesis components. The last stage of the socket production includes final trimming, plaster mold removal and other finishing operations.
- 3D printed temporary and final sockets: A digital scanner is employed to accurately capture the shape and dimensions of the residual limb, making a plaster mold unnecessary. Then, the digital model is loaded in a CAD software and the socket design is created. A structural optimization is conducted through a TO process; this phase was only carried out for the definitive socket.

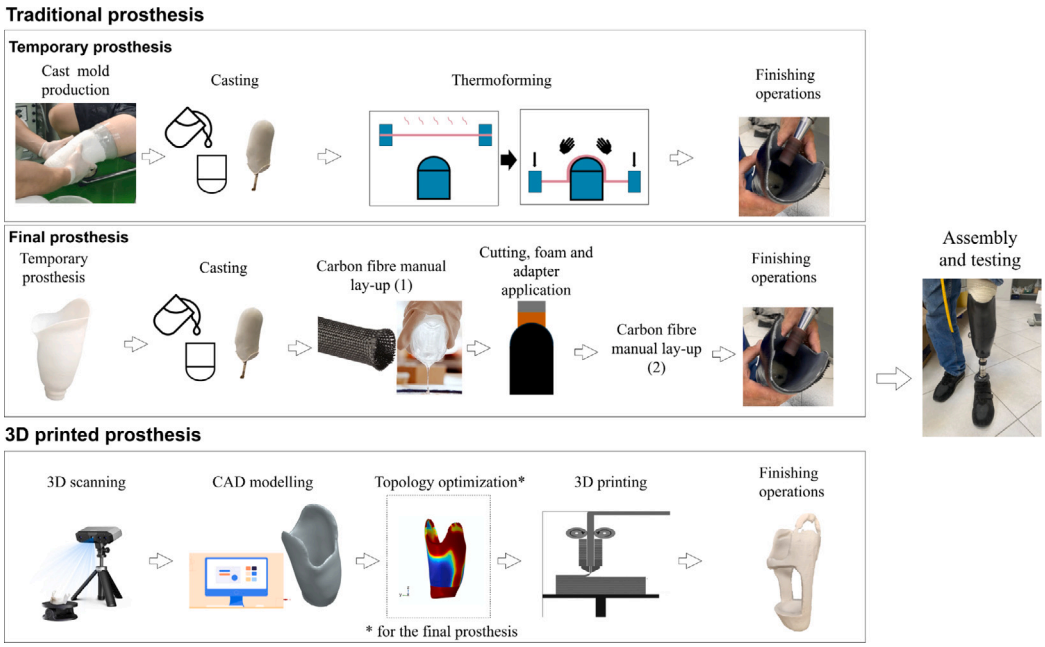

Fig. 5. Production phases for traditional 3D printed sockets for temporary and final prosthesis alternatives.

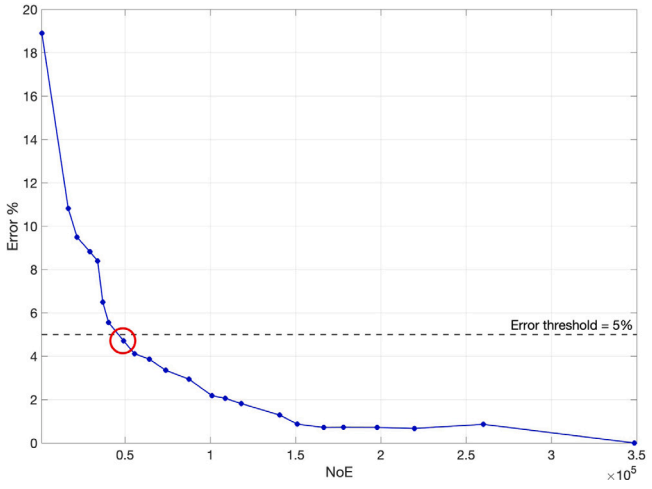

Fig. 6. Convergence analysis. Error behaviour for total strain energy versus number of elements (NoE). The red circled point identifies the mesh that has been chosen from the convergence analysis.

The model is then 3D printed using a FDM technology. For the temporary socket, polylactic acid (PLA) was selected as filament material due to its lower cost (Jones and Wilcox, 2008; Kechagias et al., 2023). On the other hand, PA12 was used for the final socket due to its higher mechanical properties. Lastly, as for the traditional alternatives, finishing operations are carried out before the complete prosthesis assembly.

In the analysis, only cost items related to the socket production were considered whilst other prosthetic components (e.g. pylon, knee and foot) were not included as they would have been the same irrespective of the considered production processes. Hence, the total cost of the prosthesis was calculated considering the different production phases, manual labour and materials costs. Data related to the traditional alternatives were provided by an industrial partner (Orthosan Srl, Italy) specialized in the field of prosthesis manufacturing. Similarly, labour cost per hour was provided by the involved company. For what concerns the innovative process, primary data related to the 3D printing processes were collected via direct measurements during the laboratory experiments (e.g. printing time, manual labour time). Scanning and CAD modelling time were retrieved from previous literature study (Van Der Stelt et al., 2021). Machines (i.e. 3D printer, workstation, 3D scanner) depreciation costs were evaluated by considering typical market purchase cost, their expected lifetime, use time, infrastructure and maintenance cost. Machine use cost per hour was calculated by considering the sum of all the incurred cost for the machines (i.e. purchase, maintenance and infrastructure) divided by the estimated uptime hours of the machines throughout their service life. In turn, uptime hours were calculated by multiplying the expected use life (in years) by the working time per year. Hence, total machines cost was calculated by multiplying the hourly cost by the required use time (Sangiorgio et al., 2025). Materials cost was quantified by multiplying the weight of the final components by the filaments costs. Machine purchase and raw material costs were derived from quotation from suppliers and company invoices. Table 2 reports the main inventory data used in the cost assessment. It is important to highlight that the CAD modelling time reported in Table 2 was estimated under the assumption that the workflow starts from a high-quality 3D scan of the residual limb, as would be the case in a real-world application where the 3D-printed socket replaces the conventional one. Modern 3D scanners are capable of producing clean and well-defined geometries, minimizing the need for extensive manual editing. The design operations, typically consisting of cleaning, trimming, and extrusion to achieve the desired thickness, can be performed quickly by experienced users. As such, a modelling time of approximately 20 min was considered reasonable and is consistent with the findings of Van Der Stelt et al. (2021), who reported similar durations for designing transtibial prostheses from residual limb scans.

3. Results

3.1. Convergence analysis

Convergence analysis was performed on the whole model using for the prosthetic socket the constitutive parameters of PA12 reported in Table 1 and adopting an h-refinement. Twenty three meshes have been tested considering an average element size $d_{avg} \in 3.3$ cm $\div$ 4 mm and

Table 2
Main inventory data employed in the cost evaluation of the traditional and innovative sockets.

Phase	Item	Quantity	Unitary cost
Traditional temporary socket			
Cast mold production	Labour	1 h	50 €/h
	Plaster bandages	2	1.7 €/unit
	Tubular bandages	1	2.95 €/unit
Plaster casting	Labour	1.5 h	50 €/h
	Plaster	1.5 kg	0.3 €/kg
Thermoforming	Labour	0.5 h	50 €/h
	Thermolyn plate	1	61.50 €
Cutting and finishing	Labour	0.5 h	50 €/h
Final traditional socket			
Plaster casting	Labour	1.5 h	50 €/h
	Plaster	1.5 kg	0.3 €/kg
Carbon fiber lay-up (1+2)	Labour	3 h	50 €/h
	CF sleeves	3 m	20 €/m
	Resin	0.6 kg	0.45 €/kg
	PVA cones	2	2.40 €/unit
	Connection system	1	260 €/unit
Cutting, plaster removal, foam	Labour	2 h	50 €/h
	Foam	0.15 kg	18.70 €/kg
	Hardner	0.15 kg	16.96 €/kg
	Pyramidal fitting	1	85 €/unit
Cutting and finishing	Labour	0.5 h	50 €/h
3D printed sockets			
Machines general data (scanner, 3D printers and workstation)	Uptime per year calculated considering 2 shifts per day (16 h tot), 200 days per year and 60% uptime.		
	Machines lifetime[a]	5 years	–
	Machines uptime per year[a]	1920 h	–
3D scanning	Labour	0.25 h	50 €/h
	Scanner purchase cost	–	10'000 €
	Scanner use time	0.25 h	1.04 €/h
CAD modelling	Labour	0.33 h	70 €/h
	Workstation purchase cost	–	2000 €
Topology optimization (final)	Labour	0.5 h	70 €/h
	Workstation use (solution time)	2.5 h	–
3D printing: temporary	3D printing machine purchase	–	2000 €
	Printing time	28.5 h	0.3 €/h
	Maintenance cost	100 €	–
	Infrastructure cost	400 €	–
	Material (PLA filament)	665.93 g	20 €/kg
	Labour	0.3 h	50 €/h
3D printing: final	3D printing machine purchase	–	12'000 €
	Printing time	22.66 h	1.51 €/h
	Maintenance cost	500 €	–
	Infrastructure cost	2000 €	–
	Material (PA12 filament)	410.39 g	50 €/kg
	Labour	0.3 h	50 €/h
Finishing operations	Labour time	0.25 h	50 €/h

[a] These values are assumed for all machines: scanner, workstation, and 3D printers.

a total number of elements $NoE \in 1213 \div 348650$. The numerical solutions from the different meshes have been compared by considering the finest FE discretization model (d_{avg} = 4 mm, NoE = 348650) as the reference solution and computing the error for each mesh in terms of total strain energy W_s. As commonly accepted (Jones and Wilcox, 2008) a converged mesh has been assumed for an error threshold of 5%. Accordingly, the behaviour of the error parameter with respect to NoE is provided in Fig. 6. The analysis highlighted that the model identified with the red circle in Fig. 6 fulfils the error estimate bound. Accordingly the chosen mesh used in the following analysis will consist of d_{avg} = 8 mm, thus resulting in a total of 48931 tetrahedral elements and 234210 degrees of freedom.

3.2. Static structural analysis

In Fig. 7, the Von Mises stress σ_{VM} distribution obtained from the static analysis is reported. Among all stress measurements, the Von Mises stress has been selected to obtain information about the load transfer mechanism and detect stress concentrations in the original non-optimized design.

3.3. Topology optimization

The results obtained from the topology optimization are shown in Fig. 8 in which is reported the topological density distribution ρ_t (top row) and the optimized design resulted from the topology optimization analysis (bottom row).

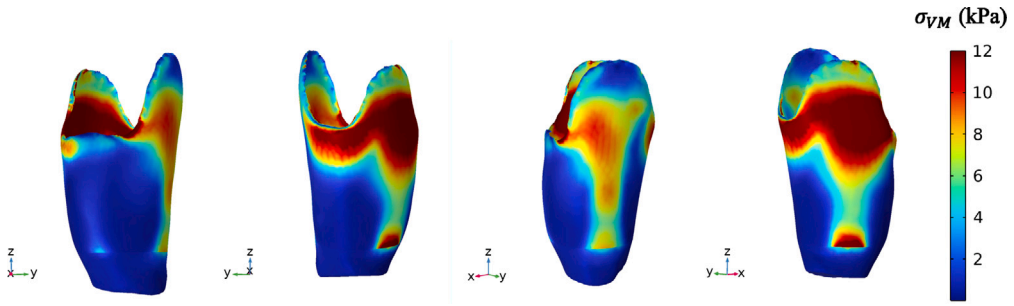

Fig. 7. Von Mises stress field in the original prosthetic socket resulting from the initial static analysis.

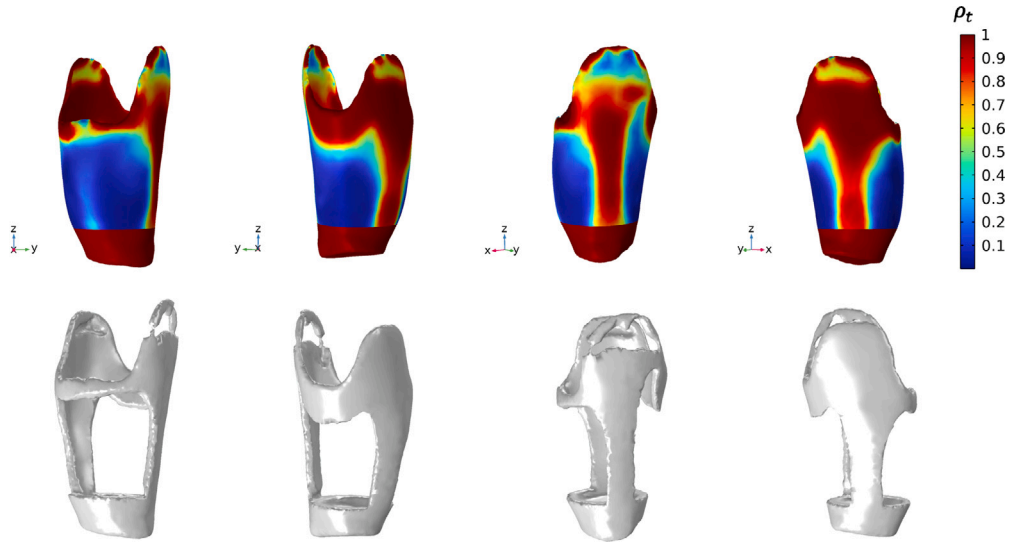

Fig. 8. Topological density (ρ_t) distribution (top) and the proposed optimal design of the prosthetic socket (bottom).

3.4. Validation

To verify the stress and displacement distributions of the optimized prosthetic socket, a validation analysis has been performed by considering the same material parameters, constitutive behaviour, loading condition and kinematic constraints of the original case. In Figs. 9 and 10 a comparison between the original prosthetic socket and the optimized design in terms of total displacement field ($\mathbf{u}_{\mathrm{TOT}}$) and Von Mises stress σ_{VM} has been shown.

3.5. 3D printing and cost assessment

Fig. 11 shows the 3D-printed version of the optimized prosthetic socket. The 3D printing time was 22 h and 40 min, significantly lower compared to the traditional technique to manufacture the transtibial socket (around 2 days according to data provided by the industrial partner). Fig. 12a shows the results of the cost assessment for the traditional and innovative processes, whereas Fig. 12b shows a breakdown of the cost of the different production phases for the 3D printed sockets. Finally, Tables 3 and 4 show the cost contribution for the traditional and 3D printed sockets.

4. Discussion

The present study focused on the application of AM with the FE-based TO to design a transtibial prosthetic socket. The Von Mises stress resulting from the static analysis provides clear insight into the load transfer mechanism in the original non optimized prosthetic socket. Specifically, the stresses are carried from the residual limb to the medial and lateral regions of the prosthetic socket, delineating a clear load path. From the TO results, it is evident that the topological density distribution follows the stress pattern. This outcome aligns with the primary objective of TO, which is to maintain material only where it is necessary and remove it from regions where it is not. As already mentioned, a comparison in terms of stress and displacement distributions was performed between the optimized and original designs to verify the effects of the topology optimization. In Fig. 9, the displacement field shows a significant modification around the superior part of the medial region of the prosthetic socket compared to the original design with a difference in terms of maximum displacement around 0.1 mm (maximum total displacement 0.14 mm in the non-optimized design vs. 0.24 in the optimized design). However, this change is consistent with the significant reduction in mass of the optimized design. It is important to highlight that except for this region, the displacement distribution in the rest of the prosthetic socket remains unchanged. Looking at the Von Mises stress distribution (Fig. 10), the optimized shape shows higher peak values compared to the original design. However, the Von Mises stress distribution seems to be more distributed across the optimized prosthetic socket than the original design, resulting in more efficient material engagement in the load transfer mechanism.

As far as the 3D printing process and cost evaluation are concerned, the innovative alternative provides relevant cost reduction with respect to the traditional ones for both the temporary (i.e. 85.8 € vs 243.3 €) and final (154.3 € vs 789.6 €) sockets. This result proves that, from an economic perspective, 3D printing can be successfully employed to substitute traditional processes; in fact, the innovative solution has a cost between a fifth (final socket) and third (temporary socket) of the traditional one. Despite requiring specialized manpower,

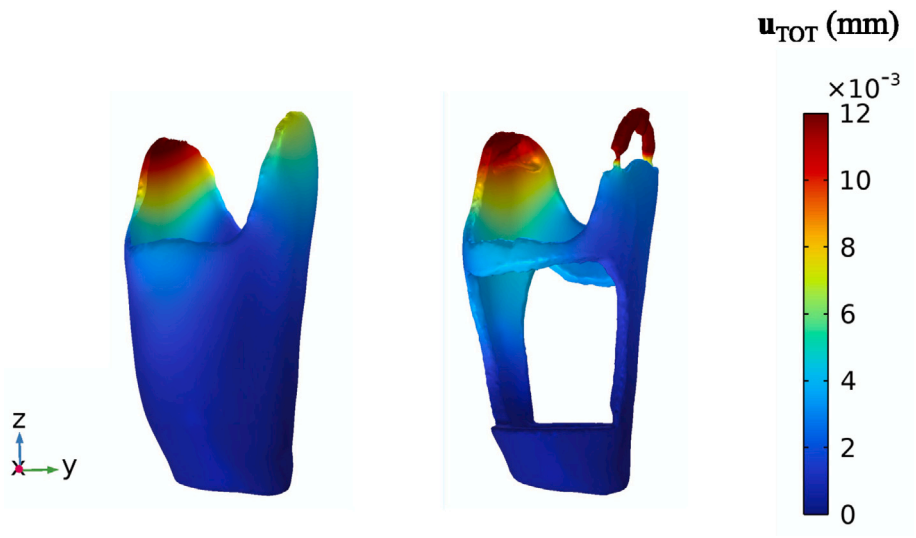

Fig. 9. Comparison between the original prosthetic socket (left) and the optimized design (right) in terms of total displacement field ($\mathbf{u}_{TOT}$ expressed in mm).

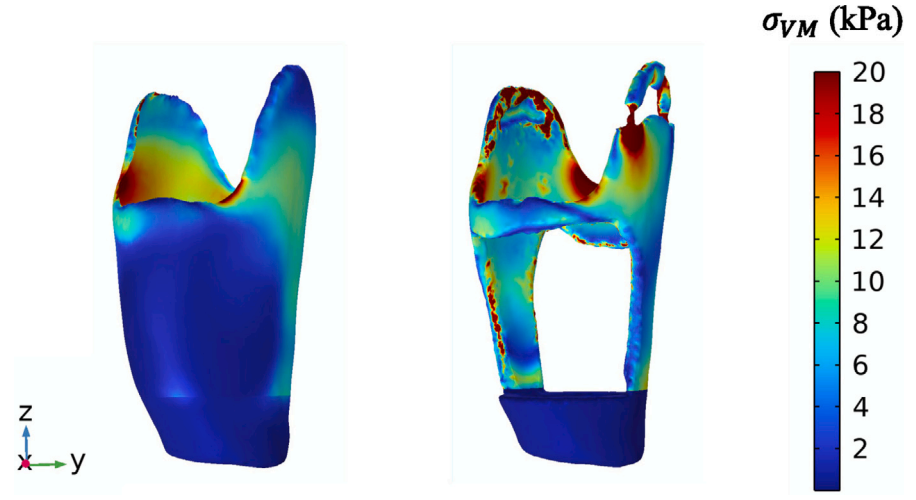

Fig. 10. Comparison between the original prosthetic socket (left) and the optimized design (right) in terms of Von Mises stress field (σ_{VM} expressed in kPa).

Table 3
Production phase costs for the traditional sockets.

Temporary traditional		Final traditional	
Production phase	Cost [€]	Production phase	Cost [€]
Cast mold production	56.35	Plaster casting in temporary prosthesis	75.44
Plaster casting	75.44	Carbon fiber manual lay-up 1	369.94
Thermoforming	86.50	Cutting, plaster removal, foam, finishing	220.65
Cutting and finishing	25.00	Carbon fiber manual lay-up 2	107.54
–	–	Cutting and finishing	25.00
TOT	**243.29**		**798.57**

Table 4
Cost breakdown for the 3D printed temporary and final sockets.

	Temporary 3D [€]	Final 3D [€]	Contributors
3D scanning	12.78	12.78	Labour and scanner use
CAD modelling	23.17	23.17	Labour and workstation use
Topology optimization	–	35.52	Labour and workstation use
3D printing	37.36	70.35	Labour, 3D printer use and raw materials
Finishing operations	12.50	12.50	Labour
Total	85.81	154.32	–

Fig. 11. 3D-Printed mockup of the prosthetic socket: (a) with printing supports and (b) after the supports removal.

production phases such as the 3D scanning and the CAD modelling are not associated with high costs. The innovative process is characterized by a high level of automation and phases that require the operator intervention are generally fast. The 3D printing phase is associated with the highest cost contribution (44%–46%); this is due to the filament cost, to machine depreciation and, to a lower extent, on labour. It is worth noting that 3D printing cost is higher for the final socket despite the lower printing time of the final component with respect to the temporary one (i.e. about 22 h vs 28 h). The PLA temporary part is characterized by low material cost (13.63 €) and, since this material is easy to print (i.e. it requires low printing temperatures and presents minimal warping) (Kechagias et al., 2023), a cheap 3D printer can be employed and low depreciation costs are obtained (8.73 €). On the other hand, for the final component, a more expensive material is used; hence, even if the amount of material used is reduced owing to the topology optimization, a higher filament cost is incurred (20.52 €). Moreover, due to higher printing temperatures and possible warping issues (Vidakis et al., 2022), a more expensive 3D printer is required to print PA, with an increment of the depreciation cost (34.83 €). The topology optimization phase of the final part accounts for about 23% of the total cost (35.52 €) mainly due to personnel cost. However, this phase allows to reduce material use and printing time; hence, a non-optimized socket produced using PA12 would have similar cost. The optimization provides benefits in terms of lightness and also allows to reduce the overall production time. The 3D printing allows to produce a complete prosthesis in just over 22 h, which can be further reduced with an appropriate selection of process parameters (e.g. by increasing printing speed or layer height) (Bianchi et al., 2022). On the other hand, according to data provided by the industrial partner, the traditional process typically requires more than 2 days for the final component production. Regarding the cost contribution of the traditional sockets, the temporary one obtained via thermoforming showed much lower costs with respect to the carbon fiber one obtained via manual lamination (243.3 € vs 798.6 €). In both cases, labour plays a significant role for the final cost, contributing for 72% (175 €) and 44% (350 €) of the total cost of the temporary and final socket, respectively. In fact, all of the production phases of the two traditional sockets rely on manpower and this yields to slow and costly production processes. This further emphasizes the advantages of an automated process such as 3D printing. Traditional processes are also associated with material waste during cutting operations, increasing production costs and environmental impacts. The carbon fiber reinforced socket has relevant material contribution due to the high unitary cost of the composite reinforcements.

An important aspect to consider is the post-processing of the geometry after TO. In this study, the topology-optimized geometry was directly manufactured without applying any smoothing operations. This choice was made to assess the feasibility of integrating TO into the design and additive manufacturing workflow for prosthetic sockets with minimal manual intervention. The study was conceived as a proof-of-concept to explore the practical applicability of this approach. Nonetheless, it is well-known that mesh-based optimization often results in surface irregularities, which may lead to stress concentrations and potentially compromise both the mechanical performance and user comfort of the final device. Therefore, smoothing operations on the CAD model could be essential to mitigate the risk of such localized stresses. From a cost perspective, considering the simplicity and short time required for basic post-processing operations, their inclusion would not significantly impact the overall manufacturing cost in the 3D printing scenarios. At the same time, these CAD modelling operations could substantially improve the surface quality and functional performance of the printed component and, at the same time, reduce the need for post printing operations.

Although the topology-optimized design allowed for a substantial reduction in material usage, the presence of large gaps in the final socket structure may compromise uniform contact and pressure distribution on the residual limb, potentially affecting patient comfort. To address this, one possible solution is to fill the gaps with a lightweight infill. Such an approach could preserve the structural efficiency achieved through TO while enhancing anatomical conformity and providing more consistent support across the entire contact surface.

The proposed work has some limitations. First, the analysis was limited to considering bonded contact between the residual limb and prosthetic socket neglecting the friction coefficient of the PA12. Additionally, only a single simplified loading condition was considered. Future studies should investigate a complete assessment of the socket's structural performance under realistic loading conditions, such as the full weight of the patient. Moreover, higher load values should be included to study high-stress scenario, suitable for evaluating the structural performance of the system under severe loading conditions (Marinopoulos et al., 2022). Analysing the system under critical conditions is essential for assessing the reliability and effectiveness of new prosthetic socket designs. Second, the objective function considered was the strain energy density and a mass reduction of 50% was prescribed. However, different objective functions and/or constraints could be explored depending on specific requirements. Third, smoothing operations after TO have not been considered, which will be addressed in future work to enhance the mechanical performance and overall quality of the prosthetic socket. Fourth, only the PA12 has been investigated. Different materials such as the Carbon PA could be examined to identify the most suitable material for manufacturing the socket. Fifth, the validation has been performed without experimental measurements. To verify the accuracy of the proposed design, experimental tests on the optimized shape are necessary. These tests will also be useful to assess the mechanical performance of the final device, both with and without smoothing operations, in order to provide a more comprehensive evaluation of the structural integrity and clinical applicability of the proposed design framework. Finally, only the FDM technology has been used for 3D printing. Different technologies such as select laser sintering (SLS) could be investigated to determine which method minimizes printing time and, consequently, reduces the overall production time.

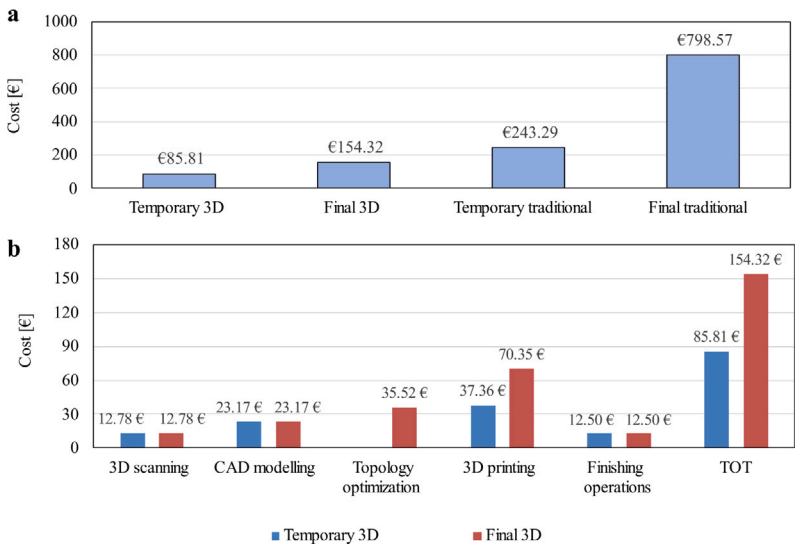

Fig. 12. Comparison between the cost of traditional and innovative prosthetic sockets (a); cost breakdown for the temporary and final 3D printed sockets (b).

5. Conclusion

This study presented an exploratory work to develop a new framework based on the combination of topology optimization and 3D printing to overcome the limitations of traditional prosthetic socket manufacturing. The goal was to assess the feasibility and potential advantages in terms of cost and manufacturing time, with the ultimate aim of replacing conventional techniques used to produce a prosthetic socket with the proposed approach.

The main results of the study indicate that significant improvements can be achieved through the proposed approach. Specifically, a potential cost reduction of approximately 80% and a decrease in manufacturing time of 50% have been estimated, demonstrating the benefits of the proposed approach. Furthermore, the results showed that the optimized shape of the prosthetic socket is able to replicate the stress and displacement fields of the original prosthetic socket. The major contribution of this work lies in demonstrating a feasible and efficient approach for prosthesis production, able to replace traditional manufacturing techniques while enhancing cost efficiency and reducing production time. Moreover, through the combination of computational modelling and analyses and 3D printing, the proposed approach represents a step forward in the development of personalized prosthetic solutions.

Overall, this proof-of-concept paves the way for future advancements in prosthetic design and production, showing that topology optimization and additive manufacturing can be successfully applied in the biomedical field to develop personalized, efficient, affordable medical devices. Future work will focus on extending the computational framework to include direct scanning of the residual limb, performing mechanical tests to investigate the mechanical performance of the original and optimized shapes and thus performing a validation of the proposed approach with respect to experimental measurements, and exploring different 3D printing technologies. Additionally, further studies will be required to assess long-term clinical performance and patient comfort, which were beyond the scope of the present work.

CRediT authorship contribution statement

Cristina Falcinelli: Writing – review & editing, Writing – original draft, Visualization, Software, Methodology, Investigation, Formal analysis, Data curation, Conceptualization. **Iacopo Bianchi:** Writing – review & editing, Visualization, Software, Methodology, Investigation, Data curation. **Alessia Carugno:** Writing – review & editing, Software, Formal analysis, Data curation. **Archimede Forcellese:** Writing – review & editing, Visualization, Supervision, Methodology, Investigation, Data curation, Conceptualization.

Declaration of competing interest

The authors declare that they have no known competing financial interests or personal relationships that could have appeared to influence the work reported in this paper.

Acknowledgements

Cristina Falcinelli acknowledges the support of the Italian National Group for Mathematical Physics (GNFM-INdAM) and the funding by the Italian Ministry of University and Research (MIUR) within the PON “Ricerca e Innovazione” 2014–2020 (azione IV.6) – FSE-REACT EU.

Data availability

Data will be made available on request.

References

Abas, M., Habib, T., Noor, S., Salah, B., Zimon, D., 2022. Parametric investigation and optimization to study the effect of process parameters on the dimensional deviation of fused deposition modeling of 3D printed parts. Polymers 14, 3667. http://dx.doi.org/10.3390/polym14173667.

Abas, M., Habib, T., Noor, S., Zimon, D., Woźniak, J., 2023. Application of multi-criteria decision-making methods in the selection of additive manufacturing materials for solid ankle foot orthoses. J. Eng. Des. 34 (8), 616–643. http://dx.doi.org/10.1080/09544828.2023.2247859, Publisher: Taylor & Francis.

Almeida, H.A., Bártolo, P.J., 2013. Topological optimisation of scaffolds for tissue engineering. Procedia Eng. 59, 298–306. http://dx.doi.org/10.1016/j.proeng.2013.05.125.

Almuflih, A., Abas, M., Khan, I., Noor, S., 2024. Parametric optimization of FDM process for PA12-CF parts using integrated response surface methodology, grey relational analysis, and grey wolf optimization. Polymers 16, 1508. http://dx.doi.org/10.3390/POLYM16111508.

Amado-Becker, A., Ramos-Grez, J., José Yañez, M., Vargas, Y., Gaete, L., 2008. Elastic tensor stiffness coefficients for SLS nylon 12 under different degrees of densification as measured by ultrasonic technique. Rapid Prototyp. J. 14 (5), 260–270. http://dx.doi.org/10.1108/13552540810907929.

Attaran, M., 2017. The rise of 3-D printing: The advantages of additive manufacturing over traditional manufacturing. Bus. Horiz. 60 (5), 677–688. http://dx.doi.org/10.1016/j.bushor.2017.05.011.

Bendsøe, M.P., Sigmund, O., 1999. Material interpolation schemes in topology optimization. Arch. Appl. Mech. (Ingenieur Archiv) 69 (9–10), 635–654. http://dx.doi.org/10.1007/s004190050248.

Bianchi, I., Forcellese, A., Mancia, T., Simoncini, M., Vita, A., 2022. Process parameters effect on environmental sustainability of composites FFF technology. Mater. Manuf. Process. 37 (5), 591–601. http://dx.doi.org/10.1080/10426914.2022.2049300.

Chojnacki, B., Chojak, A., Binek, W., Pawlik, J., Idczac, J., 2025. Accuracy of 3D printing of the samples in the prototyping of cavity-based metamaterials. Sci. Rep. 15, 13259. http://dx.doi.org/10.1038/s41598-025-98391-4.

Di Pompeo, V., Forcellese, A., Mancia, T., Simoncini, M., Vita, A., 2021. Effect of geometric parameters and moisture content on the mechanical performances of 3D-printed isogrid structures in short carbon fiber-reinforced polyamide. J. Mater. Eng Perform 30 (7), 5100–5107. http://dx.doi.org/10.1007/s11665-021-05659-7.

Ejnisman, L., Gobbato, B., De França Camargo, A.F., Zancul, E., 2021. Three-dimensional printing in orthopedics: from the basics to surgical applications. Curr. Rev. Musculoskelet Med. 14 (1), 1–8. http://dx.doi.org/10.1007/s12178-020-09691-3.

Forcellese, P., Mancia, T., Simoncini, M., Bellezze, T., 2022. Investigation on corrosion resistance properties of 17-4 PH bound metal deposition as-sintered specimens with different build-up orientations. Metals 12 (4), 588. http://dx.doi.org/10.3390/met12040588.

Hu, J., Wang, J.H., Wang, R., Yu, X.B., Liu, Y., Baur, D.A., 2019. Analysis of biomechanical behavior of 3D printed mandibular graft with porous scaffold structure designed by topological optimization. 3D Print Med. 5 (1), 5. http://dx.doi.org/10.1186/s41205-019-0042-2.

Iftekar, S.F., Aabid, A., Amir, A., Baig, M., 2023. Advancements and limitations in 3D printing materials and technologies: A critical review. Polymers 15 (11), 2519. http://dx.doi.org/10.3390/polym15112519.

Jia, X., Zhang, M., Lee, W.C., 2004. Load transfer mechanics between trans-tibial prosthetic socket and residual limb—dynamic effects. J. Biomech. 37 (9), 1371–1377. http://dx.doi.org/10.1016/j.jbiomech.2003.12.024.

Jindal, P., Prakash, P., Bassal, H., Singh, P., Din, M.A.M., Barnett, C.T., Breedon, P., 2025. Two-material-based transtibial socket designs for enhanced load-bearing capacity using FEA. Prosthesis 7 (2), 30. http://dx.doi.org/10.3390/prosthesis7020030.

Jones, A.C., Wilcox, R.K., 2008. Finite element analysis of the spine: Towards a framework of verification, validation and sensitivity analysis. Med. Eng. Phys. 30 (10), 1287–1304. http://dx.doi.org/10.1016/j.medengphy.2008.09.006.

Kam, M., Ipekci, A., Sengul, O., 2021. Investigation of the effect of FDM process parameters on mechanical properties of 3D printed PA12 samples using taguchi method. J. Thermoplast. Compos. Mater. 36, 307–325. http://dx.doi.org/10.1177/08927057211006459.

Kechagias, J.D., Vidakis, N., Petousis, M., Mountakis, N., 2023. A multi-parametric process evaluation of the mechanical response of PLA in FFF 3D printing. Mater. Manuf. Process. 38 (8), 941–953. http://dx.doi.org/10.1080/10426914.2022.2089895, Publisher: Taylor & Francis.

Kumar, R., Kumar, M., Chohan, J.S., 2021. The role of additive manufacturing for biomedical applications: A critical review. J. Manuf. Process. 64, 828–850. http://dx.doi.org/10.1016/j.jmapro.2021.02.022.

Kumar, A., Kumar, D., Faisal, N., Sharma, A., Kumar Ansu, A., Goyal, A., Saxena, K.K., Prakash, C., Kumar, D., 2024. Application of 3D printing technology for medical implants: a state-of-the-art review. Adv. Mater. Process. Technol. 10 (2), 357–372. http://dx.doi.org/10.1080/2374068X.2023.2193788, Publisher: Taylor & Francis.

Li, C.-H., Wu, C.-H., Lin, C.-L., 2020. Design of a patient-specific mandible reconstruction implant with dental prosthesis for metal 3D printing using integrated weighted topology optimization and finite element analysis. J. Mech. Behav. Biomed. Mater. 105, 103700. http://dx.doi.org/10.1016/j.jmbbm.2020.103700.

Marinopoulos, T., Li, S., Silberschmidt, V.V., 2022. AM lower-limb prosthetic socket: Using FEA for improved mechanical performance. Mater. Today: Proc. 70, 499–503. http://dx.doi.org/10.1016/j.matpr.2022.09.535.

Meng, M., Wang, J., Huang, H., Liu, X., Zhang, J., Li, Z., 2023. 3D printing metal implants in orthopedic surgery: Methods, applications and future prospects. J. Orthop. Transl. 42, 94–112. http://dx.doi.org/10.1016/j.jot.2023.08.004.

Moussa, A., Rahman, S., Xu, M., Tanzer, M., Pasini, D., 2020. Topology optimization of 3D-printed structurally porous cage for acetabular reinforcement in total hip arthroplasty. J. Mech. Behav. Biomed. Mater. 105, 103705. http://dx.doi.org/10.1016/j.jmbbm.2020.103705.

Nakonieczny, D.S., Kern, F., Dufner, L., Antonowicz, M., Matus, K., 2021. Alumina and Zirconia-reinforced polyamide PA-12 composites for biomedical additive manufacturing. Materials 14 (20), 6201. http://dx.doi.org/10.3390/ma14206201.

Nayak, C., Singh, A., Chaudhary, H., 2017. Topology optimisation of transtibial prosthesis socket using finite element analysis. International J. Biomed. Engi. . Technol. 24 (4), 323. http://dx.doi.org/10.1504/IJBET.2017.085438.

Norli, M.H.M., Sukimi, A.K.A., Ramlee, M.H., Mahmud, J., Abdullah, A.H., 2024. Static structural analysis on different topology optimization transtibial prosthetic socket leg. International J. Tech 15 (2), 455. http://dx.doi.org/10.14716/ijtech.v15i2.6711.

Pourfarzaneh, A., Taghavi, M., Helps, T., Rossiter, J., 2019. Towards adaptive prosthetic sockets using 3D-printed variable-stiffness shape-memory structures. In: 2019 2nd IEEE International Conference on Soft Robotics. RoboSoft, IEEE, Seoul, Korea (South), pp. 410–415. http://dx.doi.org/10.1109/ROBOSOFT.2019.8722811.

Prathyusha, A., Raghu Babu, G., 2022. A review on additive manufacturing and topology optimization process for weight reduction studies in various industrial applications. Mater. Today: Proc. 62, 109–117. http://dx.doi.org/10.1016/j.matpr.2022.02.604.

Sangiorgio, V., Bianchi, I., Forcellese, A., 2025. Advancing decarbonization through 3D printed concrete formworks: Life cycle analysis of technologies, materials, and processes. Energy Build. 332, 115444. http://dx.doi.org/10.1016/j.enbuild.2025.115444.

Shakiba, M., Rezvani Ghomi, E., Khosravi, F., Jouybar, S., Bigham, A., Zare, M., Abdouss, M., Moaref, R., Ramakrishna, S., 2021. Nylon—A material introduction and overview for biomedical applications. Polym. Adv. Technol. 32 (9), 3368–3383, ISBN: 1042-7147 Publisher: Wiley Online Library.

Sigmund, O., Maute, K., 2013. Topology optimization approaches: A comparative review. Struct. Multidiscip. Optim. 48 (6), 1031–1055. http://dx.doi.org/10.1007/s00158-013-0978-6.

Singh, S., Ramakrishna, S., 2017. Biomedical applications of additive manufacturing: Present and future. Curr. Opin. Biomed. Eng. 2, 105–115. http://dx.doi.org/10.1016/j.cobme.2017.05.006.

Smit, T., Koppen, S., Ferguson, S.J., Helgason, B., 2023. Conceptual design of compliant bone scaffolds by full-scale topology optimization. J. Mech. Behav. Biomed. Mater. 143, 105886. http://dx.doi.org/10.1016/j.jmbbm.2023.105886.

Sutradhar, A., Paulino, G.H., Miller, M.J., Nguyen, T.H., 2010. Topological optimization for designing patient-specific large craniofacial segmental bone replacements. Proc. Natl. Acad. Sci. USA 107 (30), 13222–13227. http://dx.doi.org/10.1073/pnas.1001208107.

Tom, T., Sreenilayam, S.P., Brabazon, D., Jose, J.P., Joseph, B., Madanan, K., Thomas, S., 2022. Additive manufacturing in the biomedical field-recent research developments. Results Eng. 16, 100661. http://dx.doi.org/10.1016/j.rineng.2022.100661.

Tomanik, M., Zmudzinska, M., Wojtkow, M., 2021. Mechanical and structural evaluation of the PA12 desktop selective laser sintering printed parts regarding printing strategy. 3D Print. Addit. Manuf. 8 (4), 271–279. http://dx.doi.org/10.1089/3dp.2020.0111.

Van Der Stelt, M., Grobusch, M.P., Koroma, A.R., Papenburg, M., Kebbie, I., Slump, C.H., Maal, T.J., Brouwers, L., 2021. Pioneering low-cost 3D-printed transtibial prosthetics to serve a rural population in Sierra Leone – an observational cohort study. EClinicalMedicine 35, 100874. http://dx.doi.org/10.1016/j.eclinm.2021.100874.

Vidakis, N., Petousis, M., Kechagias, J., 2022. Parameter effects and process modelling of polyamide 12 3D-printed parts strength and toughness. Mater. Manuf. Process. 37 (11), 1358–1369. http://dx.doi.org/10.1080/10426914.2022.2030871.

Vitali, A., Regazzoni, D., Rizzi, C., Colombo, G., 2017. Design and additive manufacturing of lower limb prosthetic socket. In: Volume 11: Systems, Design, and Complexity. American Society of Mechanical Engineers, Tampa, Florida, USA, http://dx.doi.org/10.1115/IMECE2017-71494, V011T15A021.

Wang, Y., Tan, Q., Pu, F., Boone, D., Zhang, M., 2020. A review of the application of additive manufacturing in prosthetic and orthotic clinics from a biomechanical perspective. Engineering 6 (11), 1258–1266. http://dx.doi.org/10.1016/j.eng.2020.07.019.

Zárybnická, L., Petrů, J., Krpec, P., Pagáč, M., 2022. Effect of additives and print orientation on the properties of laser sintering-printed polyamide 12 components. Polymers 14 (6), 1172. http://dx.doi.org/10.3390/polym14061172.

Zhang, G., Li, J., Zeng, H., Li, W., Wang, Q., Huang, A., 2023. Design and development of 3D-printed personalized femoral prosthesis technologies. Coatings 13 (6), 1044. http://dx.doi.org/10.3390/coatings13061044.

Zhang, M., Mak, A.F., Roberts, V., 1998. Finite element modelling of a residual lower-limb in a prosthetic socket: a survey of the development in the first decade. Med. Eng. Phys. 20 (5), 360–373. http://dx.doi.org/10.1016/S1350-4533(98)00027-7.

Zoboli, L., Bianchi, D., Falcinelli, C., Gizzi, A., 2024. Improving the manufacturing of 3D printed insoles through a combined experimental and topology optimization approach. Mech. Adv. Mater. Struct. 1–15. http://dx.doi.org/10.1080/15376494.2024.2326667.